Pretreatment ^{18}F-FAZA PET Predicts Success of Hypoxia-Directed Radiochemotherapy Using Tirapazamine

Roswitha Beck[1], Barbara Röper[2], Janette Maria Carlsen[1], Marc Cornelis Huisman[1], Julia Aloisia Lebschi[1], Nicolaus Andratschke[2], Maria Picchio[3], Michael Souvatzoglou[1], Hans-Jürgen Machulla[4], and Morand Piert[5]

[1]Clinic for Nuclear Medicine, Technische Universität München, Munich, Germany; [2]Clinic for Radiation Oncology, Technische Universität München, Munich, Germany; [3]Department of Nuclear Medicine, Scientific Institute San Raffaele, IBFM-CNR, Milan, Italy; [4]Radiopharmazie, PET Zentrum, Universität Tübingen, Tübingen, Germany; and [5]Division of Nuclear Medicine, Department of Radiology, University of Michigan, Ann Arbor, Michigan

We evaluated the predictive value of PET using the hypoxia tracer ^{18}F-fluoroazomycin arabinoside (^{18}F-FAZA) for success of radiotherapy in combination with tirapazamine, a specific cytotoxin for hypoxic cells. **Methods:** Imaging was performed on EMT6 tumor-bearing nude mice before allocating mice into 4 groups: radiochemotherapy (RCT: 8 fractions of 4.5 Gy within 4 d combined with tirapazamine, 14 mg/kg), radiotherapy alone (RT), chemotherapy alone (tirapazamine) (CHT), or control. Treatment success was assessed by several tumor growth assays, including tumor growth time from 70 to 500 μL and absolute growth delay (aGD). The median pretreatment ^{18}F-FAZA tumor-to-background ratio served as a discriminator between "hypoxic" and "normoxic" tumors. **Results:** The mean tumor growth was significantly accelerated in hypoxic control tumors (growth time from 70 to 500 μL, 11.0 d) compared with normoxic control tumors (growth time from 70 to 500 μL, 15.6 d). Whereas RT delayed tumor growth regardless of the level of hypoxia, an additive beneficial therapeutic effect of tirapazamine to RT was observed only in hypoxic tumors (aGD, 12.9 d) but not in normoxic tumors (aGD, 6.0 d). **Conclusion:** This study provides compelling evidence that hypoxia imaging using ^{18}F-FAZA PET is able to predict the success of RCT of tumor-bearing mice using the hypoxia-activated chemotherapeutic agent tirapazamine. Pretreatment ^{18}F-FAZA PET, therefore, offers a way for the individualization of tumor treatment involving radiation. The data suggest that by reserving hypoxia-directed therapy to tumors with high ^{18}F-FAZA uptake, improvement of the therapeutic ratio is possible, as the therapeutic effect of tirapazamine seems to be restricted to hypoxic tumors.

Key Words: tumor hypoxia; tirapazamine; EMT6; radiochemotherapy; FAZA

Tumor hypoxia is a common, if not characteristic, feature of many solid malignant tumors. It is related to, but not exclusively determined by, a less ordered, often chaotic and "leaky" vasculature, which can also be a feature of non-hypoxic tumors. Tumor hypoxia has the well-known effect of decreasing the sensitivity to therapeutic ionizing radiation. Therefore, it is not surprising that the response to radiation treatment decreases with the increase in the hypoxic cell fraction of solid tumors (1–3). Tumor hypoxia has also been identified as a major adverse prognostic factor that favors tumor progression and may confer resistance to pharmacologic anticancer treatment (1,4,5). Independent of these effects, hypoxia also induces genetic instability and selects for augmented tumor aggressiveness with increased metastatic potential (6,7). Hypoxia and low pH also diminish cytotoxic functions of immune cells that infiltrate a tumor. Survival of cancer cells in this abnormal microenvironment may result in local recurrence and metastatic seeds. Essentially, the abnormal tumor vasculature and the resulting abnormal microenvironment together create an effective barrier to the delivery of cancer therapy, thus diminishing anticancer treatment efficacy.

However, tumor hypoxia also constitutes a major difference between tumor and normal tissues. Thus, it presents an opportunity for therapeutic exploitation. Bioreductive drugs or hypoxia-selective cytotoxins are inactive prodrugs that are favorably activated by reductive enzymes only in the hypoxic environment of tumors (8). On activation, they release toxic metabolites that can cause cell damage and death by various mechanisms. Hypoxia-targeted chemotherapy not only supplements radiation and conventional chemotherapy (which primarily attack aerobic, proliferating cells) but also often interacts in a synergistic way with them. Therefore, a therapeutic benefit has been achieved in preclinical studies with several bioreductive drugs (9,10) and, more recently in the clinic, with the lead bioreductive drug tirapazamine (TPZ) (11–13). TPZ is a benzotriazine

with markedly increased cell toxicity under hypoxic conditions as verified in many tumor cell lines (*14*).

Thus, the identification and quantification of tumor hypoxia, preferably by noninvasive imaging, has a central role in optimizing nonsurgical cancer treatment. Recently, we evaluated the newly developed ^{18}F-labeled PET tracer fluoroazomycin arabinoside (^{18}F-FAZA) in several tumor xenograft models, including EMT6 tumors used in this study (*15*). ^{18}F-FAZA displayed a hypoxia-specific uptake mechanism and provided tumor-to-background ratios (T/B ratios) superior to that of the standard hypoxia tracer ^{18}F-fluoromisonidazole (^{18}F-FMISO). We, therefore, assessed the predictive value of ^{18}F-FAZA for hypoxia-directed treatment regimes using small animal PET. Specifically, the therapeutic success of radiotherapy, selective hypoxic-directed chemotherapy using TPZ, and the combination of both treatments was assessed.

MATERIALS AND METHODS

Radiochemistry

^{18}F-FAZA was synthesized as described previously (*16,17*). Radiochemical yields were approximately 21% at end of the beam. Typically, 7–11 GBq of ^{18}F-FAZA were isolated with a radiochemical purity of generally more than 95%.

Animals and Tumor Model

Four- to 6-wk-old female Swiss *nu/nu* mice (Charles River/Iffa Credo) were maintained at our animal care facility for 2 wk before use. The mice were housed in groups of 4 or 5 per cage in a limited access area, at a mean temperature of 23°C and a humidity of 50%–60%, and allowed food and water ad libitum. Xenografts were established from the murine breast cancer cell line EMT6 (*18*). A donor tumor was initiated by subcutaneously injecting 10^7 EMT6 tumor cells into a Swiss nude mouse. After 10 d, this tumor was harvested and transplanted subcutaneously, in pieces of approximately 1 μL, to the right lower hind limb of nude mice.

All animal experiments were performed in accordance with the guidelines for the care and use of living animals in scientific studies and the German Law for the Protection of Animals.

Treatment

Treatment was initiated after PET at a mean tumor volume of approximately 70 μL, allocating mice into 4 treatment groups: radiochemotherapy (RCT), radiotherapy alone (RT), chemotherapy alone (CHT), or control.

Specifically, for radiation or sham radiation, nonanesthetized mice were moved into a custom-built lucite cylindric restraining device with the right hind limb bearing the tumor protruding through a cut-out portion at the rear of the cylinder. The tumors were treated with 70-kV x-rays (Philips RT 100) to a round 1-cm-wide single field at a dose rate of 8.2 Gy/min and a source−skin distance of 10 cm. Eight fractions of 4.5 Gy were applied to the tumor surface at 12-h intervals twice daily within 4 d, resulting in a total dose of 36 Gy. For chemotherapy, TPZ (Sanofi-Aventis) was administered intraperitoneally (14 mg/kg body weight) 30 min before radiation or sham radiation, as this interval was shown previously as being most effective for tumor radiosensitization (*19*). Mice allocated to radiation or sham radiation without chemotherapy received intraperitoneal injections of 0.9% NaCl.

Treatment was performed on 4 consecutive cohorts of 19–25 mice each, with all tumors within a cohort derived from the same donor tumor and allocated evenly to the 4 different treatment groups. Eighty-seven tumors were included in the study.

Monitoring and Endpoint

Tumor size was assessed 3 times per week by B-mode ultrasonography using an 11-MHz transducer with a 40-mm linear probe (Logiq 500; General Electric Healthcare), which had been found to provide superior accuracy compared with caliper measurements in previous experiments (*20*). To ensure optimal contact between the plain probe and the convex tumor surface, an excess amount of ultrasound gel was used, which precluded any mechanical pressure on the tumor during the measurements. Tumor volume was estimated using the formula $V = \pi(a \times b \times c)/6$, where a, b, and c are orthogonal diameters deriving from measurements in 2 planes (along and perpendicular to the main tumor axis).

Tumors were monitored at least until volume exceeded 500 μL, and the growth time from 70 to 500 μL was calculated in days. Therapeutic success was evaluated by determining the absolute growth delay (aGD), defined as the time in days for tumors to grow from 70 to 500 μL minus the average time in days for control tumors to reach the same size. The aGD was calculated separately for tumors expressing high and low ^{18}F-FAZA uptake.

In addition, the median doubling time (Td) of untreated control tumors expressing high and low ^{18}F-FAZA uptake was calculated from the time required for control tumors to double from 200 to 400 mm^3 (usually a period of exponential growth). The log cell kill—a measure of how many proliferating tumor cells have theoretically been killed by a given treatment (expressed in orders of magnitudes by the power of 10)—was calculated from the formula:

$$\log \text{cell kill} = 0.301 \times aGD/Td, \qquad \text{Eq. 1}$$

where aGD is the median absolute growth delay for treated tumors and Td is the median doubling time of control tumors, separately for high and low ^{18}F-FAZA uptake as defined (*21*).

PET Data Acquisition, Image Reconstruction, and Data Analysis

PET was performed using a dedicated small animal scanner (MOSAIC; Philips). A full description of the prototype of this system, the A-PET system developed at the University of Pennsylvania, has been published elsewhere (*22*). Briefly, the system is based on 14,456 germanium oxyorthosilicate (GSO) crystals with dimensions of $2 \times 2 \times 10$ mm^3. The GSO crystals are glued to a continuous light guide and are read by a hexagonal array of 288 photomultiplier tubes. This gantry design leads to a port diameter of 19.7 cm, a transverse field of view (FOV) of 12.8-cm diameter, and an axial extent of 12.0 cm. The scanner operates exclusively in 3-dimensional (3D) mode. The coincidence-timing window is 12 ns; the standard energy window lies between 410 and 665 keV. Data were acquired for 12 min, resulting in a sinogram containing the detected coincidences, corrected for randoms.

During a short-inhalation narcosis, on average, 13 MBq of ^{18}F-FAZA were administered intravenously into a tail vein. Animals were kept awake with free access to food and water until PET was performed 3 h after tracer injection. Animals were anesthetized for PET by intraperitoneal injections of 70 mg/kg ketamine

(Pharmacia/Upjohn) and 7 mg/kg xylazine (Bayer). Immediately before PET, urine was removed from the bladder by catheterization using a 27-gauge plastic catheter.

Sinograms were reconstructed using the 3D Row Action Maximum Likelihood Algorithm (3D-RAMLA) (23) and a gaussian filter (2-mm full width at half maximum [FWHM]). Corrections were performed for normalization, dead time, and decay. No corrections were made for attenuation or scatter.

PET images were analyzed by drawing a thoracic background region of interest (ROI) and setting the mean plus 1 SD of the background value as the threshold for the tumor isocontour ROI. The thorax was chosen for the background ROI, as a plain muscle ROI could not be reliably delineated in muscle tissue. The T/B ratio was then calculated and used for further analyses.

Reproducibility of ^{18}F-FAZA Uptake Measurements

To assess the reproducibility of ^{18}F-FAZA uptake measurements, 2 PET scans were performed within 24 h in an additional 8 untreated animals bearing a total of 12 EMT6 tumors. Tumor sizes ranged from 47 to 343 μL. PET was performed on a microPET P4 scanner (Siemens Medical Solutions USA, Inc.), which displays a reconstructed spatial resolution from 1.8 mm at the center to 3 mm at 4-cm radial offset (24). Images were reconstructed using ordered-subset expectation maximization (OSEM) without attenuation or scatter correction, and the T/B ratio was calculated accordingly. Data analysis including ROI definitions was performed in the same manner as done on the MOSAIC scanner.

Statistical Analysis

Results are expressed as mean values of parameters ± SE. The homogeneity of group variances was assessed using the Bartlett test, selecting a conservative significance level of $P > 0.1$. To evaluate differences in tumor growh, aGD, and log cell kill between treatment groups, logarithmic data were subjected to a 2-way ANOVA taking into account the ^{18}F-FAZA uptake (above or below median) and the cross-effects between groups and using the number of animals per group as a weighting factor; this was followed by post hoc t tests. Linear regressions (±SEEs) were calculated by the least-squares method. $P < 0.05$ was considered statistically significant. Statistical tests were performed with the JMP version 5.1 statistical software package (SAS).

RESULTS

^{18}F-FAZA Distribution

Imaging revealed the expected distribution of radioactivity with low uptake in lungs, mediastinum, heart, muscle, and brain. Although large amounts of radioactivity were eliminated within the urine, bladder catheterization before imaging decreased bladder activity to acceptable levels. Also, high amounts of radioactivity were found in the gut, as ^{18}F-FAZA is metabolized in the liver and eliminated via the biliary tract (Fig. 1). Imaging was performed 3 h after tracer injection because this time point was shown previously to provide the highest T/B ratios (15).

Of 87 tumor-transplanted mice included in the study, 5 animals died before the beginning of therapy and another 12 died before reaching the endpoint of a 500-μL tumor volume. Causes of death were associated with repeated anesthesia, complications of intraperitoneal injections ($n = 1$
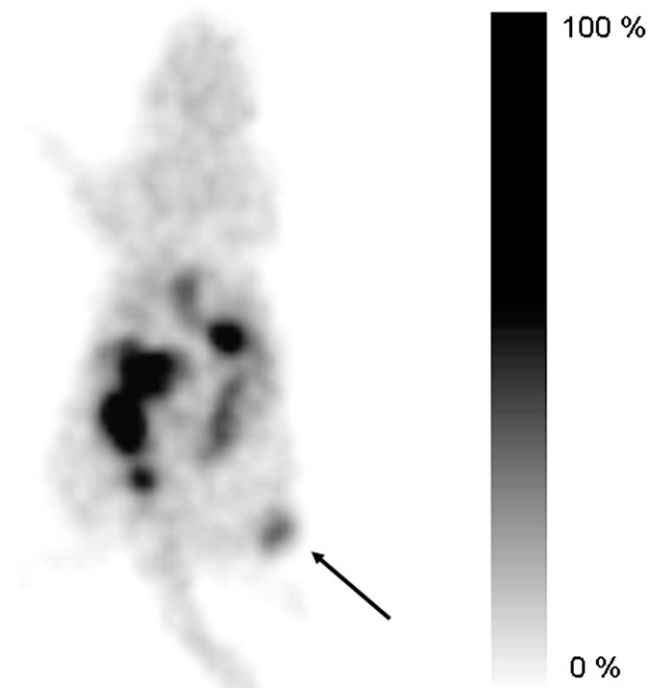

FIGURE 1. Small-animal ^{18}F-FAZA PET data were acquired 3 h after injection of 13 MBq of ^{18}F-FAZA into an EMT6 tumor-bearing (arrow) nude mouse (tumor size, 77 μL). T/B ratio was calculated as 2.52. Because of hepatic elimination of tracer, intense tracer uptake is seen in gut.

TPZ, $n = 2$ sham therapy), or general illness ($n = 4$). Another 3 tumors had to be censored because of inappropriate tumor size at ^{18}F-FAZA imaging, leaving 67 tumors for evaluation.

Among these 67 tumors, the pretreatment ^{18}F-FAZA T/B ratio was highly variable, ranging from 1.0 to 3.17 (median, 1.97). We selected the median ^{18}F-FAZA T/B ratio as discriminator for the oxygenation status of tumors. Tumors expressing ^{18}F-FAZA uptake above the median were classified as "hypoxic", whereas all other tumors were classified as "normoxic".

To assess the reproducibility of ^{18}F-FAZA uptake measurements, 12 tumors were imaged twice within 24 h in an additional 8 untreated animals. A significant linear correlation between both measurements ($y = 1.03 (\pm 0.19) x + 0.32 (\pm 0.61)$; adjusted $r^2 = 0.72$; $P < 0.001$) was found, verifying the reproducibility of the ^{18}F-FAZA T/B ratio. No significant correlation was found between the tumor weight and the ^{18}F-FAZA T/B ratio.

Tumor Growth Assays

Treatment was tolerated well for all treatment regimes. Apart from 1 abdominal skin necrosis due to accidental intracutaneous TPZ injection, no other direct toxicity of chemo- or radiotherapy was observed. Because of the tumor site at the hind leg, peripheral leg edema was a common finding with growing tumors.

Hypoxic control tumors were growing significantly faster than normoxic control tumors. Hypoxic control tumors (^{18}F-FAZA uptake above median) grew from 70 to 500 μL, on average, in 11.0 $\pm$ 1.4 d compared with normoxic control tumors growing for 15.6 $\pm$ 1.4 d; $P < 0.02$). The Td of untreated control tumors was 4 d for hypoxic and 6 d for normoxic tumors.

Treatment schemes that generally included radiation did not reduce tumor size but were followed by a noticeable growth delay. This protracted tumor growth effect was evident about 1 wk after the start of the treatment.

Treatment results are summarized in Table 1. In tumors classified as normoxic, tumor growth was significantly delayed by roughly 6–7 d after both RT and RCT. TPZ alone did not significantly alter tumor growth in comparison with normoxic controls. In tumors classified as hypoxic, RT also significantly delayed tumor growth (aGD, 7.6 d; log cell kill, 0.60), but RCT had a more profound effect delaying tumor growth to 12.9 d (log cell kill, 0.88) being significantly more effective than in normoxic tumors treated with RCT ($P < 0.05$). In addition, TPZ was found to be mildly effective in hypoxic tumors displaying a significantly better log cell kill compared with hypoxic controls ($P < 0.05$).

Figure 2 illustrates the aGD according to tumor oxygenation and treatment group. In hypoxic tumors, this difference in tumor growth delay was slightly greater than that predicted by an additive effect of drug alone (3.3 d) and radiation alone (7.6 d), suggesting a possible synergistic effect. However, even in hypoxic tumors, TPZ as a single agent (CHT) had no significant effect on tumor growth in comparison with hypoxic controls, but TPZ performed significantly better than CHT of normoxic tumors. This effect was related to the fact that normoxic tumors treated with CHT were growing slightly faster (aGD, -2.3 d) than the respective control group tumors. Also under CHT, the log cell kill for normoxic tumors was significantly worse than that of hypoxic tumors ($P < 0.05$).

Figure 3 illustrates the growth pattern in all treatment groups over the time course of the experiments. Generally, hypoxic tumors are growing faster than their normoxic counterparts, as demonstrated for controls and RT (Fig. 3A). However, this trend was reversed in treatment regimes including TPZ (Fig. 3B), with the best treatment outcome found in RCT of hypoxic tumors.

DISCUSSION

Because the decreased sensitivity of hypoxic tumors to ionizing radiation is a well-known fact, various methodologies (including increasing oxygen delivery by carbogen, erythropoetin, and hyperbaric oxygenation) have been tried to overcome radiation resistance of hypoxic tumors. However, success rates in human studies have been modest, at best (25). This could be attributed partially to increased toxicity but also, most importantly, to the lack of imaging modalities that identify suitable subjects for the initiation of hypoxia-adapted treatment regimes. More recently, bioreductive drugs such as TPZ have been used to alleviate the effects of tumor hypoxia, indicating their usefulness in animal and human studies (11,26,27). However, toxicities of TPZ can be significant (28,29). Therefore, it would be highly desirable to specifically select patients that are likely to benefit from hypoxia-adapted treatment regimes using bioreductive drugs.

We have now conducted a study evaluating the potential to stratify treatment based on hypoxia tracer uptake measurements by comparing irradiation and TPZ treatment in a well-established experimental model of tumor hypoxia (30). Previous studies on several experimental tumors have validated ^{18}F-FAZA as a promising hypoxia-imaging agent, with superior imaging characteristics compared with ^{18}F-FMISO, the standard tracer MISO. ^{18}F-FAZA displayed

TABLE 1
Tumor Growth (TG) in Normoxic and Hypoxic Tumors

Treatment group	n	TG: 70- to 500-μL volume		aGD		log cell kill	
		Days	P	Days	P		P
				Normoxic tumors			
CHT (TPZ)	7	13.3 $\pm$ 1.6		$-2.3 \pm$ 1.6		$-0.11 \pm$ 0.09	
RT (radiation)	10	22.3 $\pm$ 1.3	<0.01*	6.7 $\pm$ 1.3	<0.001*	0.34 $\pm$ 0.08	<0.02*
RCT (radiation + TPZ)	8	21.6 $\pm$ 1.6	<0.02*	6.0 $\pm$ 1.6	<0.02*	0.38 $\pm$ 0.09	<0.02*
Control (sham treatment)	9	15.6 $\pm$ 1.4		0.0 $\pm$ 1.4		0.0 $\pm$ 0.09	
				Hypoxic tumors			
CHT (TPZ)	9	14.3 $\pm$ 1.4		3.3 $\pm$ 1.4	<0.02†	0.25 $\pm$ 0.08	<0.05*, <0.01†
RT (radiation)	7	18.6 $\pm$ 1.6	<0.01*	7.6 $\pm$ 1.6	<0.01*	0.60 $\pm$ 0.1	<0.001*
RCT (radiation + TPZ)	8	23.9 $\pm$ 1.5	<0.001*	12.9 $\pm$ 1.5	<0.01*, <0.05†	0.88 $\pm$ 0.1	<0.001*, <0.01†
Control (sham treatment	9	11.0 $\pm$ 1.4	<0.02†	0.0 $\pm$ 1.4		0.0 $\pm$ 0.08	

*Significant difference between treatment and control (within groups).
†Significant difference between hypoxic and normoxic groups.
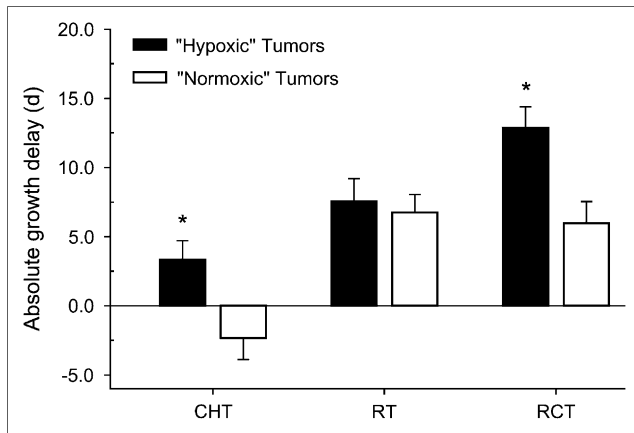Data are presented as mean $\pm$ SE.

FIGURE 2. Effect of TPZ and fractionated radiation in EMT6 tumor-volume model: absolute tumor growth delay (aGD) under treatment with TPZ alone (CHT), radiation alone (RT), and radiation + TPZ (RCT) compared with sham treatment for tumors with high and low ^{18}F-FAZA uptake (mean ± SE). Tumors displaying a pretreatment ^{18}F-FAZA T/B ratio of more than the median (1.97) were classified as hypoxic (black columns), whereas all other tumors were classified as normoxic (white columns). Compared with controls, radiation treatment in normoxic tumors and RCT in both hypoxic and normoxic tumors significantly delayed tumor growth. A more than additive treatment effect was observed for tirapazamine in combination with radiation in hypoxic tumors, but not in normoxic tumors (*$P < 0.05$ hypoxic vs. normoxic tumors).

increased retention in hypoxic tumors and correlated with independent measures of tissue oxygen tension (*15*).

Growth of sham-treated EMT6 tumors was significantly accelerated in tumors classified as hypoxic compared with normoxic tumors, indicating that tumor hypoxia as depicted by ^{18}F-FAZA PET is an independent adverse prognostic factor for tumor progression. This result as well as recent human studies using hypoxia PET in cervix, lung, and head and neck cancer patients provided evidence that noninvasive imaging based on hypoxia tracers is useful to characterize tumor biology and to predict tumor outcome after radiation treatment (*27,31,32*). These are important observations, because established alternative methods such as fine-needle electrode measurements (*1–3,5*) are technically demanding and are applicable only to superficial tumors. Most importantly, they cannot provide reliable spatial information about tumor tissue oxygenation, which would be needed to overcome hypoxia-related resistance to radiation by increasing the radiation dose to the hypoxic subvolume utilizing intensity-modulated radiotherapy (IMRT) (*33*).

In combination with irradiation, TPZ resulted in a significant prolongation of growth delay, and this therapeutic effect was restricted to tumors classified as hypoxic. Because TPZ is converted to cytotoxic metabolites only in cells experiencing significant hypoxic stress (*34*), a treatment effect of TPZ is not expected in truly normoxic tumors. However, the classification into hypoxic and normoxic tumors based on the median pretreatment T/B ratio, as done in this study, likely oversimplifies the "true" oxygenation status of tumor tissues. Studies that evaluated the spatial dis-
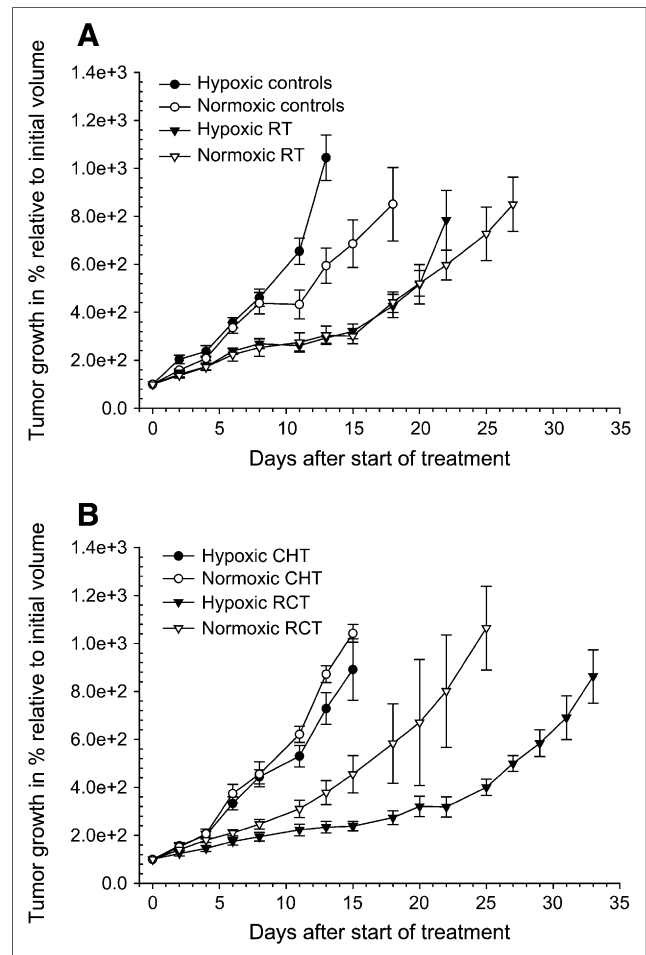

FIGURE 3. Growth curves for EMT6 tumors according to ^{18}F-FAZA uptake and treatment group. Relative median tumor growth (±SE) was plotted as a function of time after first treatment at day 0. TPZ or vehicle was given intraperitoneally twice a day for 4 consecutive days 30 min before radiation or sham radiation treatment (8 fractions of 4.5 Gy twice daily; total dose, 36 Gy). (A) Generally, hypoxic tumors (black) are growing faster than their normoxic (white) counterparts, as demonstrated for radiation treatment (RT) and controls. (B) However, this trend is reversed in treatment regimes including TPZ (CHT: TPZ as a single agent, and radiochemotherapy (RCT)), with best treatment outcome found in RCT of hypoxic tumors.

tribution of hypoxia in experimental tumors have shown that tumor oxygenation can be rather inhomogeneous (*15,35,36*). Also, even tumors displaying a T/B ratio slightly above background are expected to include variable amounts of tumor tissue hypoxia. The T/B ratio, however, is related to the amount of ^{18}F-FAZA retained within the ROI, which is influenced by the number of viable cells that accumulate the tracer as well as the accumulation rate per cell. Because ^{18}F-FAZA is known to be a hypoxia-specific marker (*15*), we can assume that a high hypoxic cell fraction within a given tumor will result in a high T/B ratio. From the standpoint of the radiooncologist, a more precise definition of the relationship between the T/B ratio and the hypoxic cell fraction would be desirable, yet it it cannot be provided

with the data acquired. Nonetheless, our results indicate that only tumors with a "significant" hypoxic fraction seem to benefit from the addition of TPZ to radiation treatment.

In this study, TPZ was given twice a day in a dose of 14 mg/kg body weight (representing 17% of the single 50% lethal dose) over 4 consecutive days, a dose that was found previously to significantly delay growth of KHT, SCCVII, and RIF-1 tumors (30). Cytotoxicity and therapeutic efficacy of TPZ were remarkably different in tumors derived from these cell lines. It had been postulated previously that the therapeutic efficacy of TPZ would be dependent on the hypoxic tumor cell fraction, which was estimated to be at 1% for RIF-1 tumors (37) and between 20% and 40% for EMT6 and SCCVII tumors (38). In fact, our results obtained from rather small groups of animals indicated a marginal beneficial effect of TPZ as a single agent in hypoxic EMT6 tumors, but not in normoxic EMT6 tumors.

However, one important aspect is the indirect dependency of the hypoxic fraction on tumor size. Therefore, a uniform distribution of tumor sizes across treatment groups, as done in this study, is essential for the assessment of treatment effects. Also, because hypoxia preferentially occurs in tumor areas surrounding necrosis (39), and because significant necrosis is inevitable at a certain tumor size, the study endpoint must be selected carefully. Tumor size measurements were performed using dedicated high-resolution ultrasound imaging in 3 dimensions, which was found to be superior to 2-dimensional caliper measurements (20). Also, ultrasound imaging allowed monitoring for the development of extensive tumor necrosis, which can be identified as regions of low signal intensity. At the selected endpoint (500-μL volume), most tumors had developed small central necrotic areas, but most of the tumor volume was confined to vital tumor tissues.

In this study, irradiation was conducted in a fractionated way, mimicking palliative treatment of human tumors. EMT6 tumors are known to be relatively radioresistant because of their significant hypoxic cell fraction. This was confirmed in a study in which even total doses of 60 Gy in single fractions of 4 Gy did not guarantee a cure in BALB/c mice bearing EMT6-tumors of 300–400 μL in size (40). In this study, we administered a total dose of 36 Gy, taking into account a smaller tumor size at study entrance (approximately 70 μL) as well as potential additional treatment effects of TPZ. The concept of 8 fractions within 4 d, each preceded by application of TPZ 30 min earlier, was adopted from earlier studies, which revealed that this time interval was most effective for tumor radiosensitization (19).

As expected, the outcome after RT was poor for hypoxic tumors in direct comparison with the better-oxygenated subgroup. But, in this setting, the difference could be explained completely by the more aggressive phenotype of hypoxic tumors, with a tumor doubling time of 4 d for hypoxic tumors and 6 d for better-oxygenated tumors. On the other hand, the aGD induced by radiotherapy was similar regardless of the level of hypoxia (7.6 and 6.7 d).

Tumor size at imaging (approximately 70 μL) was well below the spatial resolution of the MOSAIC scanner (2.7-mm FWHM in the transaxial (radial) direction and 3.4-mm FWHM in the axial direction at the center of the FOV). Therefore, partial-volume effects (resulting from measurements obtained on volumes with a linear dimension smaller than approximately twice the FWHM spatial resolution of the PET scanner in the same direction) were present for all PET measurements of tumors (41). Although partial-volume effects have influenced our measurements, these effects are not expected to result in the observed differences in ^{18}F-FAZA uptake between groups, given the fact that comparisons were made between groups of animals with rather similar tumor sizes and little variation between groups.

Because of the lack of scatter and attenuation correction on the MOSAIC scanner, absolute quantification of the ^{18}F-FAZA uptake was not possible. We calculated the ^{18}F-FAZA uptake as a ratio between tumor and normal background activity, because such a ratio is less prone to be influenced by the amount of activity injected as well as interindividual variations of the ^{18}F-FAZA metabolism (variable hepatic and renal elimination rates). Previous experiments showed that the T/B ratios yielded robust results as long as animals were awake and allowed to move freely between tracer injection and PET 3 h later (15).

To assess the reproducibility of PET measurements, we performed serial PET within 24 h in 12 untreated tumors and found a highly significant positive correlation of the ^{18}F-FAZA T/B ratio between scans. Although several factors—such as altered tumor perfusion, changes in the cellular microenvironment, and depth of anesthesia with subsequent changes in regional oxygen availability—may have influenced the results between scans, the T/B ratio appeared to be largely unaffected. Obviously, the temporal variability of ^{18}F-FAZA tumor hypoxia measurements using the T/B ratio is small within 24 h, indicating that the mean ^{18}F-FAZA T/B ratio is a reproducible measurement in tumor tissues.

Reproducibility measurements were performed on a different scanner (microPET P4 scanner) with improved spatial resolution (transaxial FWHM, 1.8 mm) compared with the MOSAIC scanner (FWHM, 2.7 mm). The microPET uses OSEM for iterative image reconstruction instead of RAMLA on the MOSAIC scanner (42). However, both algorithms have similar performance characteristics (43). To further minimize potential effects on the measurements of the T/B ratio, all images obtained from the microPET were reconstructed (as on the MOSAIC scanner) without attenuation or scatter correction, and the data analyses were performed in the same way. Because PET measurements were not compared across scanners, we consider this not critical for the purpose of reproducibility measurements.

CONCLUSION

High ^{18}F-FAZA tumor uptake was identified as an independent adverse prognostic factor for tumor progression.

TPZ resulted in a significant growth delay only in combination with irradiation, and this therapeutic effect was restricted to more severely hypoxic tumors. Although ^{18}F-FMISO PET has recently been shown to predict response to hypoxia-activated chemotherapy using TPZ in humans (27), this animal study provides—to our knowledge, for the first time—compelling evidence that the uptake of ^{18}F-FAZA is also predictive for success of RCT with TPZ. Because of its more favorable biodistribution, ^{18}F-FAZA is recommended for further preclinical and clinical testing of therapies that specifically target the hypoxic subvolume of tumors by IMRT or take advantage of the intratumoral lack of oxygen by including hypoxia-activated cytotoxins such as TPZ—especially because such treatment regimes are expected to be associated with additional toxicity and significant costs.

REFERENCES

1. Hockel M, Schlenger K, Aral B, Mitze M, Schaffer U, Vaupel P. Association between tumor hypoxia and malignant progression in advanced cancer of the uterine cervix. *Cancer Res.* 1996;56:4509–4515.
2. Molls M, Feldmann HJ, Fuller J. Oxygenation of locally advanced recurrent rectal cancer, soft tissue sarcoma and breast cancer. *Adv Exp Med Biol.* 1994;345:459–463.
3. Molls M, Stadler P, Becker A, Feldmann HJ, Dunst J. Relevance of oxygen in radiation oncology: mechanisms of action, correlation to low hemoglobin levels. *Strahlenther Onkol.* 1998;174(suppl 4):13–16.
4. Harrison LB, Chadha M, Hill RJ, Hu K, Shasha D. Impact of tumor hypoxia and anemia on radiation therapy outcomes. *Oncologist.* 2002;7:492–508.
5. Brizel DM, Dodge RK, Clough RW, Dewhirst MW. Oxygenation of head and neck cancer: changes during radiotherapy and impact on treatment outcome. *Radiother Oncol.* 1999;53:113–117.
6. Bottaro DP, Liotta LA. Cancer: out of air is not out of action. *Nature.* 2003;423:593–595.
7. Pennacchietti S, Michieli P, Galluzzo M, Mazzone M, Giordano S, Comoglio PM. Hypoxia promotes invasive growth by transcriptional activation of the met protooncogene. *Cancer Cell.* 2003;3:347–361.
8. Denny WA. Prodrug strategies in cancer therapy. *Eur J Med Chem.* 2001;36:577–595.
9. Dorie MJ, Brown JM. Modification of the antitumor activity of chemotherapeutic drugs by the hypoxic cytotoxic agent tirapazamine. *Cancer Chemother Pharmacol.* 1997;39:361–366.
10. Papadopoulou MV, Bloomer WD. NLCQ-1 (NSC 709257): exploiting hypoxia with a weak DNA-intercalating bioreductive drug. *Clin Cancer Res.* 2003;9:5714–5720.
11. Lee DJ, Trotti A, Spencer S, et al. Concurrent tirapazamine and radiotherapy for advanced head and neck carcinomas: a phase II study. *Int J Radiat Oncol Biol Phys.* 1998;42:811–815.

12. Miller VA, Ng KK, Grant SC, et al. Phase II study of the combination of the novel bioreductive agent, tirapazamine, with cisplatin in patients with advanced non-small-cell lung cancer. *Ann Oncol.* 1997;8:1269–1271.
13. von Pawel J, von Roemeling R, Gatzemeier U, et al. Tirapazamine plus cisplatin versus cisplatin in advanced non-small-cell lung cancer: a report of the international CATAPULT I study group—Cisplatin and Tirapazamine in Subjects with Advanced Previously Untreated Non-Small-Cell Lung Tumors. *J Clin Oncol.* 2000;18:1351–1359.
14. Wouters BG, Wang LH, Brown JM. Tirapazamine: a new drug producing tumor specific enhancement of platinum-based chemotherapy in non-small-cell lung cancer. *Ann Oncol.* 1999;10(suppl 5):S29–S33.
15. Piert M, Machulla H-J, Picchio M, et al. Hypoxia-specific tumor imaging with ^{18}F-fluoroazomycin arabinoside. *J Nucl Med.* 2005;46:106–113.
16. Reischl G, Ehrlichmann W, Bieg C, Kumar P, Wiebe LI, Machulla H-J. Synthesis of ^{18}F-FAZA, a new tracer for hypoxia [abstract]. *J Nucl Med.* 2002;43(suppl):364P.
17. Reischl G, Ehrlichmann W, Bieg C, et al. Preparation of the hypoxia imaging PET tracer [^{18}F]FAZA: reaction parameters and automation. *Appl Radiat Isot.* 2005;62:897–901.
18. Rockwell SC, Kallman RF, Fajardo LF. Characteristics of a serially transplanted mouse mammary tumor and its tissue-culture-adapted derivative. *J Natl Cancer Inst.* 1972;49:735–749.
19. Papadopoulou MV, Ji M, Bloomer WD. Schedule-dependent potentiation of chemotherapeutic drugs by the bioreductive compounds NLCQ-1 and tirapazamine against EMT6 tumors in mice. *Cancer Chemother Pharmacol.* 2001;48:160–168.
20. Röper B, Beck R, Andratschke N, et al. Volumetry of experimental tumors: advantage of ultrasound compared to standard approaches [in German] [abstract]. *Strahlenther Onkol.* 2005;181:103.
21. Papadopoulou MV, Ji M, Bloomer WD, Hollingshead MG. Enhancement of the antitumor effect of cyclophosphamide with the hypoxia-selective cytotoxin NLCQ-1 against murine tumors and human xenografts. *J Exp Ther Oncol.* 2002;2:298–305.
22. Surti S, Karp JS, Perkins AE, et al. Imaging performance of A-PET: a small animal PET camera. *IEEE Trans Med Imaging.* 2005;24:844–852.
23. Daube-Witherspoon M, Matej S, Karp J, Lewitt R. A row-action alternative to the EM algorithm for maximizing likelihoods in emission tomography. *IEEE Trans Nucl Sci.* 2001;48:24–30.
24. Tai C, Chatziioannou A, Siegel S, et al. Performance evaluation of the microPET P4: a PET system dedicated to animal imaging. *Phys Med Biol.* 2001;46:1845–1862.
25. Corry J, Rischin D. Strategies to overcome accelerated repopulation and hypoxia: What have we learned from clinical trials? *Semin Oncol.* 2004;31:802–808.
26. Emmenegger U, Morton GC, Francia G, et al. Low-dose metronomic daily cyclophosphamide and weekly tirapazamine: a well-tolerated combination regimen with enhanced efficacy that exploits tumor hypoxia. *Cancer Res.* 2006;66:1664–1674.
27. Rischin D, Hicks RJ, Fisher R, et al. Prognostic significance of [^{18}F]-misonidazole positron emission tomography-detected tumor hypoxia in patients with advanced head and neck cancer randomly assigned to chemoradiation with or without tirapazamine: a substudy of Trans-Tasman Radiation Oncology Group Study 98.02. *J Clin Oncol.* 2006;24:2098–2104.
28. Rischin D, Peters L, Hicks R, et al. Phase I trial of concurrent tirapazamine, cisplatin, and radiotherapy in patients with advanced head and neck cancer. *J Clin Oncol.* 2001;19:535–542.
29. Craighead PS, Pearcey R, Stuart G. A phase I/II evaluation of tirapazamine administered intravenously concurrent with cisplatin and radiotherapy in women with locally advanced cervical cancer. *Int J Radiat Oncol Biol Phys.* 2000;48:791–795.
30. Brown JM, Lemmon MJ. Potentiation by the hypoxic cytotoxin SR 4233 of cell killing produced by fractionated irradiation of mouse tumors. *Cancer Res.* 1990;50:7745–7749.
31. Dehdashti F, Grigsby PW, Mintun MA, Lewis JS, Siegel BA, Welch MJ. Assessing tumor hypoxia in cervical cancer by positron emission tomography with [60]Cu-ATSM: relationship to therapeutic response—a preliminary report. *Int J Radiat Oncol Biol Phys.* 2003;55:1233–1238.
32. Eschmann SM, Paulsen F, Reimold M, et al. Prognostic impact of hypoxia imaging with ^{18}F-misonidazole PET in non-small cell lung cancer and head and neck cancer before radiotherapy. *J Nucl Med.* 2005;46:253–260.
33. Grosu AL, Piert M, Weber WA, et al. Positron emission tomography for radiation treatment planning. *Strahlenther Onkol.* 2005;181:483–499.
34. Stratford IJ, Workman P. Bioreductive drugs into the next millennium. *Anticancer Drug Des.* 1998;13:519–528.

35. Obata A, Yoshimoto M, Kasamatsu S, et al. Intra-tumoral distribution of ^{64}Cu-ATSM: a comparison study with FDG. *Nucl Med Biol.* 2003;30: 529–534.

36. Sorensen M, Horsman MR, Cumming P, Munk OL, Keiding S. Effect of intratumoral heterogeneity in oxygenation status on FMISO PET, autoradiography, and electrode Po_2 measurements in murine tumors. *Int J Radiat Oncol Biol Phys.* 2005;62:854–861.

37. Brown JM, Twentyman PR, Zamvil SS. Response to the RIF-1 tumor in vitro and in C3H/Km mice to X-radiation (cell survival, regrowth delay, and tumor control), chemotherapeutic agents, and activated macrophages. *J Natl Cancer Inst.* 1980;64:605–611.

38. Moulder JE, Rockwell S. Hypoxic fractions of solid tumors: experimental techniques, methods of analysis, and a survey of existing data. *Int J Radiat Oncol Biol Phys.* 1984;10:695–712.

39. Beck R, Picchio M, Haubner R, et al. Intratumoral distribution and correlation of ^{18}F-FAZA, ^{125}I-gluco-RGD and HIF-1 expression in a murine tumor hypoxia model [abstract]. *J Nucl Med.* 2005;46(suppl):126P.

40. Greer S, Schwade J, Marion HS. Five-chlorodeoxycytidine and biomodulators of its metabolism result in fifty to eighty percent cures of advanced EMT-6 tumors when used with fractionated radiation. *Int J Radiat Oncol Biol Phys.* 1995;32: 1059–1069.

41. Hoffman EJ, Huang SC, Phelps ME. Quantitation in positron emission computed tomography. 1. Effect of object size. *J Comput Assist Tomogr.* 1979;3:299–308.

42. Lamare F, Turzo A, Bizais Y, Le Rest CC, Visvikis D. Validation of a Monte Carlo simulation of the Philips Allegro/GEMINI PET systems using GATE. *Phys Med Biol.* 2006;51:943–962.

43. Hwang D, Zeng GL. A new simple iterative reconstruction algorithm for SPECT transmission measurement. *Med Phys.* 2005;32:2312–2319.